Int J Earth Sci (Geol Rundsch) (2011) 100:1533–1550
DOI 10.1007/s00531-010-0568-4

ORIGINAL PAPER

The metamorphic aureole of the Nisa-Alburquerque batholith (SW Iberia): implications for deep structure and emplacement mode

Luís González Menéndez · Antonio Azor · Alvaro Rubio Ordóñez · Isabel Sánchez-Almazo

Received: 31 July 2009 / Accepted: 2 June 2010 / Published online: 22 June 2010
© Springer-Verlag 2010

Abstract The Nisa-Alburquerque granitic batholith (southern Variscan Belt, Iberian Peninsula) has been studied by petrological, structural and geophysical approaches, obtaining contrasting models for its deep structure and emplacement sequence. In order to test these models and gain knowledge on the thermal increase induced by the intrusion, we have studied its contact aureole, which was developed in similar country rock lithologies (mica schists alternating with metasandstones and feldespatic schists) all along the northern external contact of the batholith. Our results indicate no change in metamorphic grade and some variations in aureole width, which narrows toward the western sectors of the batholith. Cordierite is the only contact metamorphic mineral developed together with a high temperature biotite probably related to the granite thermal input. By considering these new data, together with zircon saturation temperatures within the granite and previous petrological and geophysical studies, we propose a model in which the feeder zones of the granitic magmas were an eastern main one and a western secondary one. We have also made comparisons of the metamorphic grade in the country rocks and the xenoliths within the granite. Most of the xenoliths have the same metamorphic facies as the country rocks (Crd-zone), though some of them contain slightly different assemblages (And + Crd), which could be explained in different ways: (1) differences in the primary schist compositions, (2) increased time-span of xenoliths in contact with the melt and (3) xenolith incorporation at slightly higher depths during final granite ascent.

Keywords Variscan granitoids · Contact metamorphism · Cordierite · Andalusite · Xenoliths

L. G. Menéndez (✉)
Instituto Geológico y Minero de España, Parque Científico, Av. Real 1, 24006 León, Spain
e-mail: lgonm@unileon.es

A. Azor
Departamento de Geodinámica, Facultad de Ciencias, Universidad de Granada, Campus de Fuentenueva, 18002 Granada, Spain
e-mail: azor@ugr.es

A. R. Ordóñez
Departamento de Geología, Área de Petrología y Geoquímica, Universidad de Oviedo, C/Jesús Árias de Velasco, 33005 Oviedo, Asturias, Spain
e-mail: arubio@geol.uniovi.es

I. Sánchez-Almazo
CEAMA, Universidad de Granada, Junta de Andalucía, Av Mediterráneo, 18006 Granada, Spain
e-mail: sanchez@ugr.es

Introduction

The southwestern Iberian Peninsula is a region formed mainly by Late Proterozoic and Paleozoic rocks deformed during the Variscan Orogeny in Late Palaeozoic times. The Iberian Variscan Belt has been divided into different domains as shown in Fig. 1 (Lotze 1945; Julivert et al. 1972; Farias et al. 1987; Arenas et al. 1988). There are two external fold-and-thrust-belts located to the NE (Cantabrian Zone, CZ) and to the SW (South Portuguese Zone, SPZ), and four internal zones where metamorphic and magmatic rocks crop out: Ossa-Morena Zone (OMZ), Central Iberian Zone (CIZ), West-Asturian Leonese Zone (WALZ) and Galicia-Tras os Montes Zone (GTMZ). The contacts among these Variscan domains are usually faults or shear zones. One of the main features of the internal zones of the

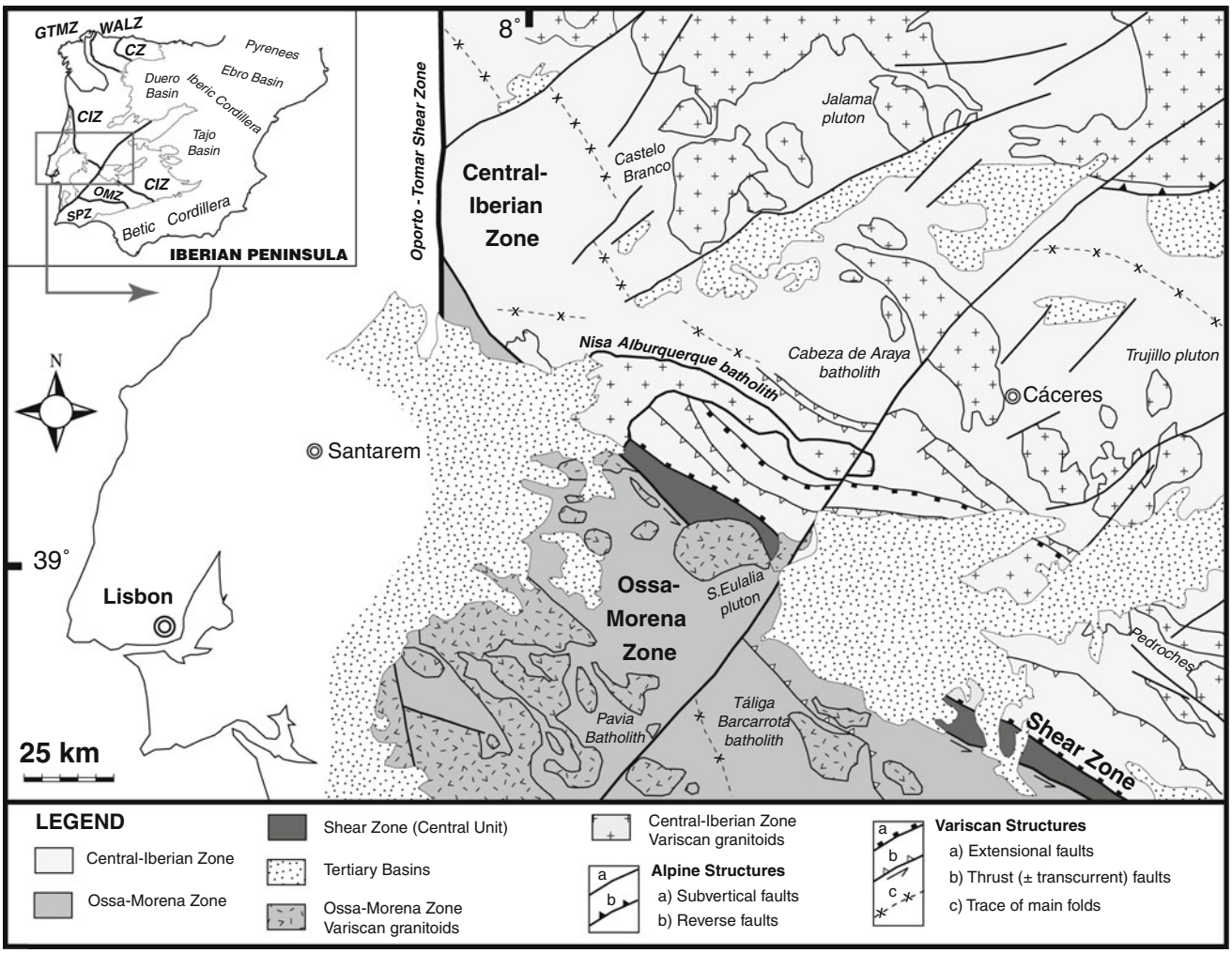

Fig. 1 Simplified geological map of the Central-Southwestern Iberian Peninsula, based and modified from the Tectonic Map of Spain (Rodríguez Fernández et al. 2004). The Nisa-Alburquerque batholith is located in the central part of the figure. Names of some other plutons and batholiths are stated. Variscan domains are: *CZ* Cantabrian Zone, *WALZ* West-Asturian Leonese Zone, *CIZ* Central Iberian Zone, *GTMZ* Galicia-Tras os Montes Zone, *OMZ* Ossa-Morena Zone, *SPZ* South Portuguese Zone

Variscan Orogen in the Iberian Peninsula is the abundance of granitoid rocks, most of which are Variscan to late Variscan (Upper Carboniferous) granodiorites and granites. These granitoid rocks are widespread over the OMZ, CIZ and GTMZ with a net decrease in abundance in the WALZ and toward the two external orogenic zones. OMZ Variscan granitoids are moderately peraluminous to metaluminous and slightly different from those in the CIZ, where moderate to high peraluminous types dominate (Bea et al. 1987; Castro et al. 2002; Bea 2004; Casquet and Galindo 2004; Galindo and Casquet 2004). The study of these granitoids has made important recent advances concerning geochronology, petrogenetic processes and emplacement dynamics. Nevertheless, issues related to emplacement and deep internal structure of granites are controversial and difficult to establish due to the absence of detailed studies of the magmatic fabrics and the common lack of important reliefs that would allow 3D structural relationships to be observed. In order to overcome these difficulties, a number of geophysical approaches have been applied to gain knowledge about the deep structure of granite plutons and batholiths. Combined gravimetric and magnetometric studies have been carried out to investigate the composition and geometry of granite body roots, while magmatic fabric data from Anisotropy of Magnetic Susceptibility measures and phenocryst orientation were made to decipher emplacement dynamics (e.g., Vigneresse and Bouchez 1997; Aranguren et al. 1997, 2003; Yenes et al. 1999; Simancas et al. 2000; Galadí-Enríquez et al. 2003; Romeo et al. 2006). These studies were made in several plutons and batholiths from the CIZ and OMZ with significant results regarding the main roots or feeder zones. In the present work, our approach to gain knowledge about the deep structure and emplacement mode of the Nisa-Alburquerque batholith is focussed on the variations of the contact metamorphic facies and aureole thickness

variations. Comparison of these data with zircon saturation temperatures of the granites and with results of previous geophysical studies suggests a deep structure of the batholith defined by two roots (at the eastern and western zones) and a middle zone where magmas from both sources encountered and accumulated. Within the granite, xenoliths with different metamorphic assemblages occur (cordierite vs cordierite + andalusite) suggesting different hypothesis of origin that will be discussed.

Rationale

The Late Variscan Nisa-Alburquerque granite batholith is roughly located in the limit between the CIZ and OMZ (Fig. 1). Previous geological data indicated that the main root or feeder zone of granitic magma was located in the western domains of the batholith: intrusive relationships of some granitic units, western location of less differentiated members of the granitic units, etc. (González Menéndez 1998; Solá 2007). On the contrary, geophysical data (gravimetry + magnetometry) suggests that the main root is located in the eastern zones of the batholith, with westward decreasing granite thickness (Campos and Plata 1991; Azor et al. 2000; Gumiel et al. 2002). In order to match geological and geophysical data, an intermediate solution was considered but some kind of independent test is required to check if any one of the two hypotheses (geological versus geophysical) is more reasonable. To do so, we have studied variations in the thickness and metamorphic grade of contact aureole all along the length of the batholith. Our approach is focused on field geology and petrography, aided by a mineral chemistry and geochemical study, of the contact aureoles of the Nisa-Alburquerque batholith to look for zones of the country rocks with higher temperature record. The size and metamorphic grade in a contact aureole is supposed to be dependent on several factors (Yardley 1989; Bucher and Frey 2002) namely: (1) size and temperature of the intrusion, (2) latent heat of magma crystallization, (3) initial temperature of country rock, (4) thermal conductivity and diffusivities of country rock, (5) water content and permeability of country rock, (6) heat consumed in metamorphic reactions. The rationale of our study is that country rock zones affected by high magma volume and/or high magma temperature would develop a wider contact aureole. The temperature reached by the country rocks is mainly dependent on initial temperature of the magmas and country rocks (Jaeger 1968). Size of intrusion may be important in this respect because it will determine the time that the country rocks are being heated by the intrusive magmas. Given the low rates of metamorphic reactions (Baxter 2003), the time that the country rocks are exposed to the magma heat will determine whether or not reactions progress in a substantial amount. Because metamorphic facies is defined by a given metamorphic assemblage, both temperature (magmas and country rocks) plus heating time, directly related to the intrusion size, are the most important factors to reach a specific metamorphic facies.

In a batholith or pluton, temperature distribution of the magmas will be mainly dependent on the initial temperature of the magma batches plus the loss of heat toward the country rocks. Where a root zone continuously feeds up the magma chamber with new batches, one can expect to find higher magma temperatures than in other loci of the magma chamber with no feeder roots. In the sectors without roots, the magma loses heat toward the country rocks in all directions, including the floor. This hypothesis is corroborated by the good correlation found between the position of probable roots of the batholith deduced from gravimetric studies (Azor et al. 2000) and the highest values of zircon saturation temperatures, considered to represent an estimate of magma temperatures at the time of emplacement (González Menéndez 1998).

Therefore, we expect to correlate greater aureole development (metamorphic facies and extension of the contact metamorphism) with higher magma volume (intrusion size) and temperature, which, in turn, would coincide with the main magma feeder zones. In the Nisa-Alburquerque batholith, the country rocks more suitable for this type of study are located along the northern contact, where mica schists with alternating feldspathic schists, quartzites and metasandstones crop out. These rocks are grouped in the so-called Schist–Greywacke Complex of Upper Neoproterozoic to Lower Cambrian age (Rodríguez Alonso et al. 2004). As shown in Figs. 1 and 2, the batholith intruded this unit all along its northern contact, which is subparallel to the structural anisotropy in the region. In the studied zone, the temperature gradient related to regional metamorphism of Variscan age (which is affecting lower Carboniferous rocks and is older than 300–310 Ma granitic rocks of the area) is low and perpendicular to the main structures. No variations of pre-intrusion metamorphism were observed along strike. Accordingly, we can assume that factors: 3, initial temperature of country rocks, 4, thermal conductivity and diffusivity, and 5, water content and permeability of country rocks, were probably similar all along the northern contact of the batholith. Regarding factors 2, latent heat of magma crystallization, and 6, heat consumed in metamorphic reactions, we observed little along-strike variation since we find no significant differences in the mineralogical assemblages both in the granite and in the country rocks. By considering these assumptions, we can expect that main variations (thickness + metamorphic facies) in the thermal aureole

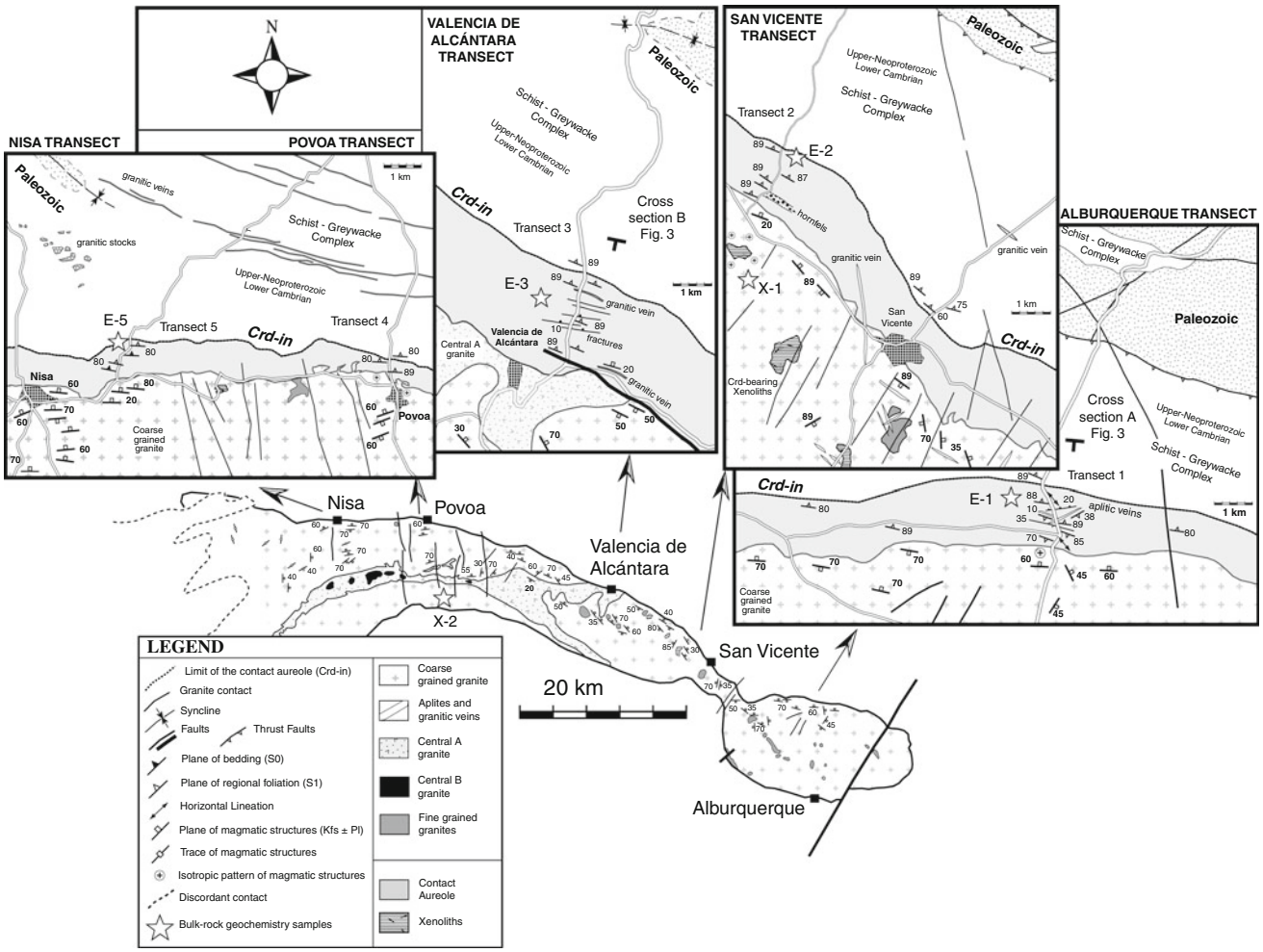

Fig. 2 Detailed geological map sketches of the Nisa-Alburquerque batholith and its northern contact aureole, where the different transects were made. Petrographic samples were taken at the same points where structure orientations were measured. Maximum aureole widths are found in the middle and eastern parts of the batholith

along the northern contact of the Nisa-Alburquerque batholith have been mainly dependent on factor 1, the size and temperature of the intrusion. Therefore, these conditions would permit us to study and sample the effects of magma intrusion along country rock lithologies of similar composition, physical properties and initial P–T conditions in a 90 km-long east–west transect.

The Nisa-Alburquerque batholith and its country rocks

The Nisa-Alburquerque batholith is emplaced in the southwestern part of the CIZ, very close to its boundary with the OMZ (Fig. 1). This boundary is a 3–10-km-wide shear zone (Azor et al. 2004; Simancas et al. 2001), though in the area of study its limits are not well defined. The part of Nisa-Alburquerque batholith located within the CIZ runs parallel to this shear zone. Toward the west, the batholith cuts across this shear zone and intrudes the OMZ rocks. Rb–Sr datings indicate an intrusion age of 294 ± 11 Ma (González Menéndez 2002). Recent U–Pb SHRIMP data from Solá (2007) and Solá et al. (2009) indicate an emplacement age of 309–307 Ma. By considering the complete record of radiometric ages obtained by different authors across the W-E length of the batholith, a possible age difference between the western domains with a mean age of 300 Ma and the eastern domains with a mean age of 289 Ma has been suggested (González Menéndez 1998). The Nisa-Alburquerque batholith is composed of peraluminous monzogranites and leucogranites, which can be grouped into four main granitic units (Fig. 2): (1) coarse-grained granite (2) central granite A, (3) fine-grained granite and (4) central granite B. The most widespread granitic unit, which hosts all of the other ones, is the coarse-grained granite. This facies is composed of porphyritic ± equigranular leucogranites and monzogranites with biotite (Bt) + muscovite (Ms) ± cordierite (Crd) ± tourmaline (Tur) ± andalusite (And) (mineral abbreviations according to Kretz 1983). The most common accessory

minerals are apatite (Ap) + zircon (Zrn) + monazite (Mnz) + ilmenite (Ilm) ± rutile (Rt) ± xenotime (Xe) ± uraninite (Ur). K-feldspar (Kfs) and plagioclase (Pl) phenocrysts show shape orientations, thus allowing the internal magmatic structure of the batholith to be mapped (Fig. 2). This magmatic fabric tends to be concordant with the general shape of the batholith. No clear subsolidus fabrics have been found. The rest of the granitic units appear as intrusions (central granite A, central granite B, fine-grained granites) and/or magmatic enclaves (some of the fine-grained granites) hosted by the coarse-grained granite. All the granitic units have a similar composition to the coarse-grained granite, with the exception of the central granite B, which is made up of monzogranites and granodiorites (±tonalites) with Bt ± hornblende (Hbl) ± titanite (Tnt). The geochemistry and isotopic composition also corroborate these differences (González Menéndez 2002; González Menéndez and Bea 2004; Solá 2007; Solá et al. 2009).

Regional metamorphism has affected northern country rock formations giving place to the development of a low-grade greenschist assemblage with Bt + Ms + chlorite (Chl) + quartz (Qtz) + albite (Ab), which corresponds to the Chl–Bt zone (López-Munguira et al. 1991). The metamorphic grade related to this regional metamorphism does not change along the zone where the Nisa-Alburquerque batholith intruded. The country rocks show primary features such as bedding (S_0) and a penetrative regional foliation (S_1), which corresponds to the D_1 Variscan event. Foliations related to later deformational phases are observed locally. Where both types of structures ($S_1 + S_0$) can be observed, they are subparallel. Cordierite spots developed in response to the thermal input from the granite are post-tectonic and overprint the regional cleavage. At map scale, the country rock orientations are parallel or subparallel to the batholith contact and also subparallel to the magmatic fabrics within the granite. Nonetheless, at outcrop scale, the granite contact is somewhat oblique in some places to the country rock orientations and to the internal magmatic structure. In any case, the batholith contact with the country rocks is vertical or subvertical.

Previous research in the northern contact aureole has been focussed on the central and eastern domains of the batholith (Rodríguez Suárez 1985). These studies described contact metamorphic assemblages with Crd and Crd ± And in the higher-grade zones. The inferred P–T conditions were 2.3 kbar and 500°C. In the present work, we did not find andalusite, neither in the country rock aureole nor in most of the xenoliths studied. González Menéndez and Azor (2003) considered the existence of a primary mineral assemblage with Ms + And + Tur in the granite, thus proposing somewhat higher pressure conditions for granite emplacement (~2.3–3 kbar). As for temperature estimates, González Menéndez (1998) and González Menéndez and Azor (2003) established a final magma temperature of 650°C based on zircon saturation temperatures. Based on this same analytical data set, we have constructed a contour map with zircon saturation temperatures (see further ahead in the text) with the idea of comparing the estimated magma temperature with the loci of feeder roots obtained from previous gravimetric studies. These data are also used to compare the spatial relationships of magma temperature with country rock metamorphic grade and aureole thickness.

Methods

In order to study possible along-strike variations in the contact aureole, we have selected five north–south transects along the northern boundary of the batholith. Each transect starts inside the batholith and continues northward into the country rocks. We have established several stations along the transects where we have collected samples and recorded the following data:

Distance from the granite contact, lithology, observed mineralogy, orientation of the different structures and presence or absence of granitic, pegmatitic and/or quartz dikes. Finally, thin sections were obtained from the samples to study in detail textures and mineral assemblages with optical and scanning electron microscopy (IGME: Spain's Geological Survey and CEAMA: Centro Andaluz de Medio Ambiente, Granada, Spain). Mineral chemistry (Tables 1, 2, 3) was obtained using a Cameca SX 100 microprobe equipped with five wavelength-dispersive spectrometers (Servicios Científico-Técnicos, Oviedo University, Spain), operating at 20 nA electron beam current, 15 kV accelerating voltage and 10 s counting time for all elements, except F, Cl (15 s) and P (30 s). Analytical data of country rock and granite geochemistry are presented in Tables 4 and 5. These data consist of major elements and Zr. The major elements were determined by X-ray Fluorescence (XRF), while Zr was measured by both XRF and Inductively Coupled Plasma Mass Spectrometry (ICP-MS) (Granada University, Spain). The complete chemical data set and used analytical conditions are in Ramírez and Menéndez (1999).

Results

A general study of petrography, mineral chemistry and whole-rock geochemistry of the contact aureole has been done along the five transects of the northern contact of the batholith (Fig. 2). The contact between the granite and the country rocks (Schist–Greywacke Complex) was usually difficult to find in outcrops. Where seen, the contact is sharp and steeply dipping (80°–90°) outward or inward the

Table 1 Microprobe analyses of selected biotites from country rocks (Alb) and xenoliths (X-1)

Biotite Bt type	ALB11d Type-II	ALB11f Type-II	X-1b Type-II	X-1c Type-II
SiO_2	42.98	39.41	34.85	34.57
Na_2O	0.09	0.10	0.19	0.13
MgO	5.33	6.18	10.04	9.47
Al_2O_3	20.72	20.63	19.91	19.74
K_2O	7.79	7.63	7.82	8.43
CaO	0.09	0.08	0.05	0.00
TiO_2	2.26	2.32	1.88	2.05
MnO	0.03	0.01	0.08	0.00
FeO	14.90	15.61	19.25	20.52
Total	94.57	92.35	94.30	95.04
Si	3.11	2.96	2.64	2.63
Al_4	0.88	1.03	1.35	1.37
Al_6	0.87	0.78	0.42	0.40
Ti	0.12	0.13	0.10	0.11
Fe^{3+}	0.00	0.01	0.11	0.10
Fe^{2+}	0.91	0.96	1.10	1.19
Mn	0.00	0.00	0.00	0.00
Mg	0.57	0.69	1.13	1.07
Ca	0.00	0.00	0.00	0.00
Na	0.01	0.01	0.02	0.01
K	0.72	0.73	0.75	0.81
X_{Mg}	0.38	0.41	0.50	0.47

Biotite Bt type	X-1d Type-II	X-1e Type-II	X-1f Type-II	X-1 g Type-II	X-1 h Type-I
SiO_2	35.84	34.55	35.79	34.99	36.58
Na_2O	0.21	0.15	0.16	0.25	0.14
MgO	8.75	8.85	9.36	9.40	10.46
Al_2O_3	20.08	19.74	20.14	20.84	19.93
K_2O	8.50	8.73	8.75	8.78	8.85
CaO	0.00	0.00	0.01	0.00	0.00
TiO_2	2.25	2.96	2.07	2.18	1.35
MnO	0.05	0.12	0.02	0.09	0.06
FeO	21.21	20.00	19.14	19.86	19.11
Total	97.24	95.56	95.78	96.67	97.01
Si	2.66	2.62	2.68	2.61	2.70
Al_4	1.33	1.37	1.31	1.38	1.29
Al_6	0.43	0.39	0.46	0.45	0.44
Ti	0.12	0.17	0.11	0.12	0.07
Fe^{3+}	0.09	0.06	0.07	0.06	0.09
Fe^{2+}	1.22	1.20	1.13	1.17	1.09
Mn	0.00	0.00	0.00	0.00	0.00
Mg	0.97	1.00	1.04	1.04	1.15
Ca	0.00	0.00	0.00	0.00	0.00
Na	0.03	0.02	0.02	0.03	0.02
K	0.80	0.84	0.83	0.83	0.83
X_{Mg}	0.44	0.45	0.48	0.47	0.51

Table 2 Microprobe analyses of selected cordierites from xenoliths (X-1)

Cordierite	X-1a	X-1b	X-1i	X-1k	X-1l	X-1m	X-1n	X-1o
SiO_2	48.27	48.12	48.74	47.42	48.48	48.66	48.81	48.43
TiO_2	0.00	0.00	0.00	0.02	0.00	0.00	0.00	0.00
Al_2O_3	34.22	33.97	34.52	35.08	34.81	33.90	33.72	34.42
FeOt	9.38	9.16	9.21	9.31	9.04	8.40	8.75	8.56
MnO	0.14	0.16	0.17	0.23	0.11	0.25	0.26	0.21
MgO	7.24	7.06	7.15	7.14	7.05	7.17	7.09	7.25
CaO	0.00	0.01	0.00	0.00	0.00	0.01	0.00	0.00
Na_2O	0.68	0.82	0.68	0.69	0.91	0.94	0.99	0.73
K_2O	0.00	0.01	0.00	0.01	0.00	0.01	0.06	0.00
Total	100.02	99.37	100.50	99.93	100.40	99.40	99.73	99.64
Si	4.88	4.89	4.90	4.79	4.87	4.93	4.93	4.90
Al	4.08	4.07	4.09	4.18	4.12	4.05	4.02	4.10
Ti	0.00	0.00	0.00	0.00	0.00	0.00	0.00	0.00
Fe^{2+}	0.79	0.77	0.77	0.78	0.76	0.71	0.74	0.72
Mn	0.01	0.01	0.01	0.02	0.01	0.02	0.02	0.01
Mg	1.09	1.07	1.07	1.07	1.05	1.08	1.07	1.09
Ca	0.00	0.00	0.00	0.00	0.00	0.00	0.00	0.00
Na	0.13	0.16	0.13	0.13	0.17	0.18	0.19	0.14
K	0.00	0.00	0.00	0.00	0.00	0.00	0.00	0.00
X_{Mg}	0.57	0.57	0.57	0.57	0.57	0.59	0.58	0.59
Na + K	0.13	0.16	0.13	0.13	0.17	0.18	0.20	0.14

batholith. The preferred mineral orientation of the magmatic phenocrysts tends to be subparallel to this contact. Nevertheless, in some locations (near Alburquerque), the contact plane has usually similar strike to the magmatic fabric but higher dips.

Regarding the mineralogy from other domains of the Central Iberian Zone (CIZ) where the Schist–Greywacke Complex is described with very low grade or no metamorphic imprint, its mineral assemblage is formed by Qtz + Ab + white mica (Ms) + Chl ± clay minerals: ± Kln ± smectite (López-Munguira et al. 1990). Country rock schists developed their initial metamorphic mineral assemblage as a result of the Variscan regional metamorphism that structured a biotite-chlorite regional metamorphic zone (Bt-Chl zone). The reaction involved could have been $Ms + Chl \rightarrow Bt + Ms + Qtz + H_2O$ (I) (Mather 1970). The contact metamorphic sequence typical of pelitic aureoles at low pressures is formed by five metamorphic zones (Yardley 1989, and references therein), where cordierite appears as the first distinctive index mineral formed by the discontinuous reaction of $Chl + Ms + Qtz \rightarrow Crd + Bt + H_2O$ (II). This reaction is thought to be responsible for the development of cordierite spots in the slates. In the area of study, we consider the appearance of cordierite as the external boundary of the contact aureole. The thermal aureole is thus at the cordierite zone and we do

Table 3 Microprobe analyses of selected muscovites (Ms), tourmalines (Tur) and feldspars from country rocks (Alb) and xenoliths (X-1)

Ms	Alb11	Alb11	Tur	Alb11
SiO_2	47.12	46.67	SiO_2	37.04
TiO_2	0.72	0.56	TiO_2	0.35
Al_2O_3	34.60	34.50	Al_2O_3	32.03
FeO	0.86	0.76	FeO	8.42
MnO	0.00	0.00	MgO	5.76
MgO	0.51	0.55	CaO	0.07
CaO	0.02	0.04	Na_2O	2.11
Na_2O	0.41	0.42	K_2O	0.02
K_2O	9.27	9.34	B_2O_3	10.00
Total	93.55	92.89	Total	96.05
Si	3.15	3.14	Si	6.10
Ti	0.03	0.02	Ti	0.04
Al_4	0.84	0.85	Alt	0.00
Al_6	1.88	1.89	Al_Z	5.99
Fe^{3+}	0.00	0.00	Al_Y	0.23
Fe^{2+}	0.04	0.04	Ti	0.04
Mg	0.05	0.05	Fe	1.22
Ca	0.00	0.00	Mg	1.49
Na	0.05	0.05	Ca	0.01
K	0.79	0.80	Na	0.71

Feld.	Alb-11	X-1	X-1	X-1	X-1
SiO_2	65.07	66.35	65.53	65.35	64.83
TiO_2	0.02	0.01	0.00	0.03	0.00
Al_2O_3	17.97	22.91	22.54	21.96	22.35
Cr_2O_3	0.02	0.00	0.04	0.02	0.00
FeO_t	0.14	0.16	0.26	0.58	0.20
MgO	0.01	0.00	0.00	0.07	0.00
MnO	0.00	0.00	0.01	0.00	0.00
CaO	0.01	1.15	1.14	1.09	1.10
Na_2O	1.26	10.53	10.60	10.63	10.71
K_2O	13.98	0.07	0.07	0.07	0.05
Total	98.48	101.17	100.18	99.81	99.24
Si	12.11	11.61	11.57	11.56	11.56
Al	3.94	4.72	4.69	4.58	4.69
Fe	0.02	0.02	0.04	0.09	0.03
Mg	0.00	0.00	0.00	0.02	0.00
Mn	0.00	0.00	0.00	0.00	0.00
Cr	0.00	0.00	0.01	0.00	0.00
Ca	0.00	0.11	0.11	0.10	0.10
Na	0.46	3.57	3.63	3.64	3.70
K	3.32	0.02	0.02	0.02	0.01
Ab	12.08	96.65	96.69	96.81	96.94
An	0.02	2.92	2.87	2.74	2.74
Or	87.90	0.44	0.44	0.45	0.31

not find any other metamorphic zone, such as the andalusite, lower sillimanite and upper sillimanite zones. The exception is found in a few xenoliths that show And + Crd assemblages.

Studies based on different contact aureoles of metapelitic composition (Pattison and Harte 1997; Pattison et al. 2002; Pattison and Vogl 2005) indicate that the stability of mineral assemblages in some of the different metamorphic zones (i.e. Crd-zone, [Crd + And]-zone, And-zone) can vary more with pressure than with temperature because the reaction Ms + Crd → And (or Al_2SiO_5) + Bt + Qtz + H_2O has a low negative slope in the P–T space. In this scheme, the lower P-assemblage would be the Crd-zone, followed at slightly higher pressures by [Crd + And] and the And-zones. Isobaric heating at a very specific pressure and constant whole-rock Mg/(Mg + Fe) composition would also be able to generate a sequence of Crd → Crd + And → And, as temperature increases.

N–S transects

(1) The first transect was made in the eastern domain where the batholith has an elliptical shape of ~20 × 10 km. This transect started at the northern contact, within the granite. At this sector, the granite (coarse-grained facies) has a distinctive mineral assemblage containing Bt + magmatic Crd + Tur + And. At some small outcrops, the assemblage Bt + Tur can be dominant. Just at the external granite contact, the feldspars show no preferred mineral orientation, though nearby these phenocrysts run parallel or subparallel to the granite contact, showing high dips (Figs. 2 and 3a). Small-sized pegmatite and aplitic dikes are common. The first country rocks close to the granite contact are schists and quartzites. The country rock fabric consists in a very penetrative foliation that has a N110°–120°E strike and very steep dip to the SW or NE. A secondary subtle foliation is observed in relation to kink bands affecting the principal foliation (Fig. 3a). These later structures could have been formed in relation to granite emplacement. At the middle of this transect, there is a sector with aplitic granite intrusions and late fracturing. Within the country rock schists, the mineral assemblage observed is Qtz + Bt-I + Crd + Bt-II (± Tur) ± Ms ± Ab. This assemblage occurs in most outcrops of the metamorphic aureole along this transect (Fig. 3a). The main modal variations observed are a cordierite decrease in metasandstone or quartzite beds and a Bt-II ± Tur increase toward the granite contact. The presence of two different biotite generations (Bt-I and Bt-II) could be related to an initial Bt-I development during the regional metamorphism

Table 4 Major element contents (wt%) from selected country rocks and xenoliths. The metamorphic index mineral from each sample is indicated in the table. Location of samples in Fig. 2

Sample Type Index min.	E-1 Country rock Crd	E-2 Country rock Crd	E-3 Country rock Crd	E-5 Country rock Crd	X-1 Xenolith Crd	X-2 Xenolith Crd + And
SiO_2	73.03	71.22	62.62	67.9	58.11	51.8
Al_2O_3	13.55	14.39	18.60	15.97	20.01	27.5
Fe_2O_3	4.69	5.30	6.64	4.95	7.94	8.46
MnO	0.04	0.04	0.04	0.01	0.05	0.04
MgO	1.26	1.73	2.11	1.34	2.76	1.87
CaO	0.44	0.23	0.23	0.08	0.39	0.19
Na_2O	1.81	2.54	2.51	0.84	2.48	0.21
K_2O	2.49	2.49	3.39	3.50	4.01	4.62
TiO_2	0.71	0.70	0.94	0.79	0.94	1.17
P_2O_5	0.14	0.17	0.15	0.10	0.23	0.16
LOI	1.69	1.38	2.12	3.71	2.71	3.71
Tot	99.85	100.19	99.36	99.19	99.63	99.73
X_{Mg}	0.21	0.24	0.24	0.21	0.25	0.18

Table 5 Bulk rock composition of granitic rocks from the Nisa-Alburquerque batholith (coarse-grained granite): Major element contents (wt%), Zr contents (ppm), Aluminium Saturation Index (ASI) and calculated Zircon Saturation Temperatures: T°C (Zr)

Sample	ALL 17	ALL 20	ALL 19	ALL 22	ALL 21	ALL 24	ALL 25	ALL 23	ALL26	ALL27	ALL28
SiO_2	76.95	74.00	75.60	73.32	74.73	75.09	73.53	75.37	72.89	71.51	74.18
Al_2O_3	12.75	14.02	13.24	13.82	13.54	13.27	13.54	12.91	14.14	14.73	13.66
CaO	0.43	0.43	0.45	0.54	0.49	0.55	0.65	0.51	0.64	0.68	0.51
Na_2O	3.29	3.66	3.6	3.77	3.80	3.67	3.5	3.48	3.80	3.96	3.67
K_2O	4.11	4.75	4.26	4.9	4.29	4.39	4.77	4.27	5.18	5.25	4.39
Zr (ppm)	54	36	51	56	39	55	74	49	55	57	55
ASI	1.19	1.17	1.16	1.10	1.14	1.12	1.12	1.15	1.08	1.09	1.18
T(Zr)°C	715	681	707	708	686	710	731	703	704	706	712

Sample	ALL 29	ALL 33	ALL 34	ALL 35	ALL 36	ALL 37	ALL 15	ALL 41	ALL 42	ALL 44	ALL 45	ALL 47
SiO_2	75.61	75.89	74.70	76.40	73.93	75.34	75.22	74.68	75.59	75.77	74.47	73.43
Al_2O_3	13.34	12.82	13.10	12.66	13.42	13.02	13.16	13.19	13.23	12.65	13.05	13.59
CaO	0.36	0.54	0.56	0.44	0.57	0.44	0.40	0.49	0.52	0.60	0.59	0.64
Na_2O	3.66	3.46	3.47	3.30	3.51	3.53	3.27	3.56	3.60	3.31	3.23	3.40
K_2O	4.02	4.44	4.49	4.37	4.60	4.27	4.39	4.49	4.47	4.41	4.65	4.97
Zr(ppm)	47	50	76	43	58	61	45	62	59	62	79	73
ASI	1.21	1.11	1.13	1.15	1.13	1.15	1.21	1.13	1.13	1.11	1.14	1.12
T(Zr)°C	704	703	735	695	714	720	701	719	715	719	739	729

Sample	ALL 49	ALL 50	ALL 51	ALL 52	ALL 67	ALL 75	ALL 71	ALL 66	ALL 73	ALL 60	ALL 61	ALL 59
SiO_2	74.29	71.73	71.94	70.67	68.56	73.80	72.74	73.80	76.37	73.64	71.87	69.46
Al_2O_3	13.04	1.41	14.28	15.21	15.75	14.49	14.35	15.15	13.09	14.67	13.84	15.78
CaO	0.60	0.92	0.80	0.82	1.54	0.47	0.58	0.75	0.32	0.60	0.77	1.06
Na_2O	3.28	3.68	3.79	4.08	3.60	3.60	3.71	3.37	3.53	3.44	3.26	3.34
K_2O	4.69	5.05	5.13	5.52	4.92	4.72	4.62	5.70	4.67	4.98	5.03	6.09
Zr (ppm)	85	78	96	55	96	52	52	102	30	74	108	117
ASI	1.12	1.07	1.07	1.07	1.12	1.21	1.18	1.15	1.14	1.20	1.13	1.12
T(Zr)°C	743	729	745	700	744	710	707	755	668	736	760	761

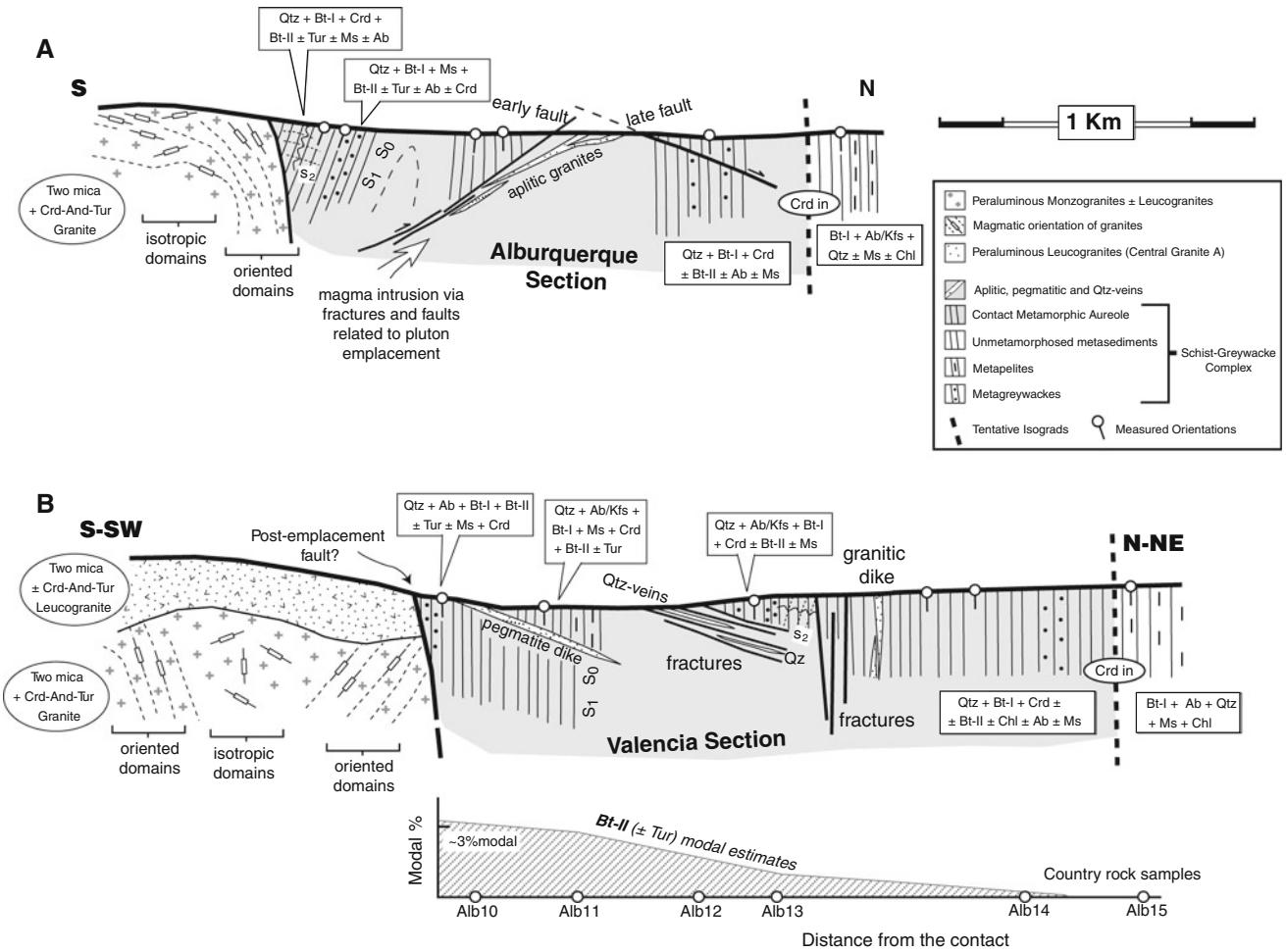

Fig. 3 Schematic N–S cross-sections interpreted from transects 1 (Alburquerque, **a**) and 3 (Valencia de Alcántara, **b**). Vertical scale is not included trying to outline the main lithologic, metamorphic, magmatic and structural relationships. In both cross-sections the metamorphic assemblage is shown, from the outer to the inner contact aureole. In section **b**, an approximated modal % estimation of the association Bt-II ± Tur was made using thin sections from the country rock samples. See text for further explanations

(dark brown biotites) and a Bt-II formation event during the contact metamorphism (small sub-idiomorphic yellow–brown biotites). Cordierite appears as pseudomorphs with occasionally some traces of fresh metamorphic cordierite at their cores. These pseudomorphs usually show an external corona made up of Bt-I + Bt-II ± Tur, while some of them are completely replaced by Bt-II + Tur. The cordierite pseudomorphs are disposed over previous microfolds described by the main mica-rich assemblage of the rock (Bt + Ms). Away from the granite contact, cordierite content shows little modal decrease until reaching distances of ~1.8–1.9 km, where it suddenly disappears. Therefore, this distance is taken here as the external limit of the contact aureole.

(2) The second transect was performed ~10 km to the west of transect 1 (Fig. 2). It started within the coarse-grained granite, composed at this location of Bt + Ms + Crd. The granite shows a weak preferred mineral orientation (Kfs), defining a magmatic fabric with N110°E strike and 10–20° dip toward the NE. In the country rocks, the regional foliation strikes N120° and dips 80–90° to the NE. The schists close to the granite contact show porphyroblast pseudomorphs very similar to the ones observed in transect 1, thus corresponding probably to cordierite. Apart from the pseudomorphs, the assemblage is made up of Qtz + Bt + Ms + Bt-I + Bt-II. At 350 m from the granite contact, a distinctive hornfels layer with the same kind of porphyroblast pseudomorphs appears. Further away from the granite contact, we observed schists with the same assemblage of cordierite pseudomorphs, until reaching a distance of 1.6 km from the contact, where no more trace of porphyroblasts is observed.

(3) The third transect was made from Valencia de Alcántara to the north (Fig. 2). We started again inside the granite, which corresponds here to the central facies A (peraluminous two-mica leucogranite with scarce cordierite phenocrysts at this locality). We observed no preferred mineral-shape orientation within this granite. Toward the

east, the coarse-grained granite crops out, showing K-feldspar orientation dipping at high angles toward the granite interior. The external granite contact crosscuts both the magmatic fabric and the internal granite contacts (Figs. 2 and 3b). This fact suggests that the external contact here could be a fault as depicted in Fig. 2. Toward the north, away from the granite, the first country rocks to crop out are hornfelsic schists with porphyroblasts very similar to the ones described above. The fabric in these rocks is a NE steeply dipping foliation with N110°E strike. The schists are made up of Qtz + Bt-I + Ms + Crd ± Bt-II ± Tur ± Ab ± Kfs, with a high modal content of cordierite porphyroblasts. Type-II biotite has ~2–3% modal abundance close to the granite contact and continually decreases toward the N (Fig. 3b). In the middle part of this transect, quartz dikes oriented parallel to the main foliation are observed. A small granitic vein was located somewhat further to the north. Kink microfolds with associated crenulation cleavage were observed in this part of the transect. At a distance of 2.6 km from the granite contact, the absence of cordierite pseudomorphs marks the end of the contact aureole.

(4) The fourth transect was made at the locality of Povoa e Meadas. Starting within the coarse-grained granite, we have observed a small stock of fine-grained granite located close to the contact. Both granitic facies have a distinctive mineralogy with Bt + Ms and show no preferred mineral orientation. In the country rocks, the regional foliation strikes N90–95°E and dips steeply to the N. The first country rocks to crop out close to the granite contact are hornfelsic schists. All along the transect, the schists have a mineral assemblage composed of Qtz + Bt-I + Ms + Crd ± Bt-II ± Ab/Kfs and are crowded with cordierite porphyroblasts in the mica-rich layers. At a distance of ~600 m from the granite contact, the modal abundance of porphyroblasts decreases importantly. At ~800 m from the granite contact, the aureole ends.

(5) The fifth transect is located in Nisa (Fig. 2). The granite here corresponds to the coarse-grained facies with a distinctive mineral assemblage of Bt + Crd. Muscovite is very rare at this location. K-feldspar and plagioclase phenocrysts show a magmatic fabric striking N93°E and dipping 20° to the N. However, the magmatic fabric dips very variably in this area. In the country rocks, the regional foliation strikes N93–112°E and dips steeply to the NE. Horizontal crenulation cleavage overprinting the regional foliation is observed.

The country rocks (Qtz + Bt-I +Ms + Crd ± Bt-II ± Feldspars) close to the granite contact are hornfelses with porphyroblasts probably representing, as in all previous transects, cordierite pseudomorphs. Away from the granite contact, the schists continue to show porphyroblasts with only a slight decrease in modal abundance. The aureole ends at a distance of ~1.2 km from the granite.

Petrography and mineral assemblages in the contact aureole

In all of the studied cross-sections, the lithologies close to the granite contact are usually hornfelses, while the rest of the outcropping aureole is made up of porphyroblast-bearing spotted schists. Mineral and textural features shown in Fig. 4a, b and c correspond to transect 3 (Valencia de Alcántara) and are considered to be representative of all transects. The microphotographs show relationships between cordierite porphyroblasts and regional foliation. Cordierite appears as patchy porphyroblasts overprinting the regional foliation of the country rocks, thus indicating post-tectonic growth with respect to the Variscan deformation. Nonetheless, porphyroblasts have in most cases an elliptical shape that could be due to some later flattening affecting the country rocks. This later flattening might be related to late intrusive magma pulses, which could have promoted some batholith growth by ballooning processes (Ramsay 1989). In this regard, the late intrusion of central granites A and B in the Central-Western sectors of the Nisa-Alburquerque batholith, as well as fine-grained granites in the eastern sectors, provide some evidence in favor of such ballooning processes. Moreover, the dominant granitic facies (coarse-grained granite) is probably also composed by several magmatic pulses successively intruded into the main magma mush.

Both country rock lithologies, hornfelses and spotted schists, are mainly composed of Qtz + Bt (I + II) + Ms ± Ab (± Kfs) ± Tur. Most of the porphyroblasts are cordierite pseudomorphs made up of sericite ± Chl ± Tur (Fig. 4a, b, c). No assemblage with Crd + And was observed in the samples collected. The feldspar observed is mainly albite, while K-feldspar occurs rarely and without any spatial relationship to the granite contact, thus being considered as preserved detritic K-feldspar. No traces of fibrolite were observed in any sample. The two different types of biotite recognized are shown in more detail in Fig. 4c. Although both types are quite similar, type-II shows a yellowish color under microscope parallel polarizers and somewhat higher relief. Type-I biotites seem to be more aligned with the foliation bands compared to type-II. These data suggest that the crystallization of type-II biotites post-dated type-I. Most cordierite porphyroblasts in the country rocks have an outer corona rich in Bt-II + Bt-I ± Tur crystals. Development of type-II biotite coronas around cordierite porphyroblasts indicates a probable synchronous growth related to reaction (II) Ms + Chl + Qtz → Crd + Bt-II + H_2O. The modal content of type-I biotite in cordierite coronas is similar or lower than in the matrix, which indicates that it is not related to cordierite growth. Cordierite pseudomorphs completely replaced by Bt-II ± Tur have also been observed. Type-II biotite

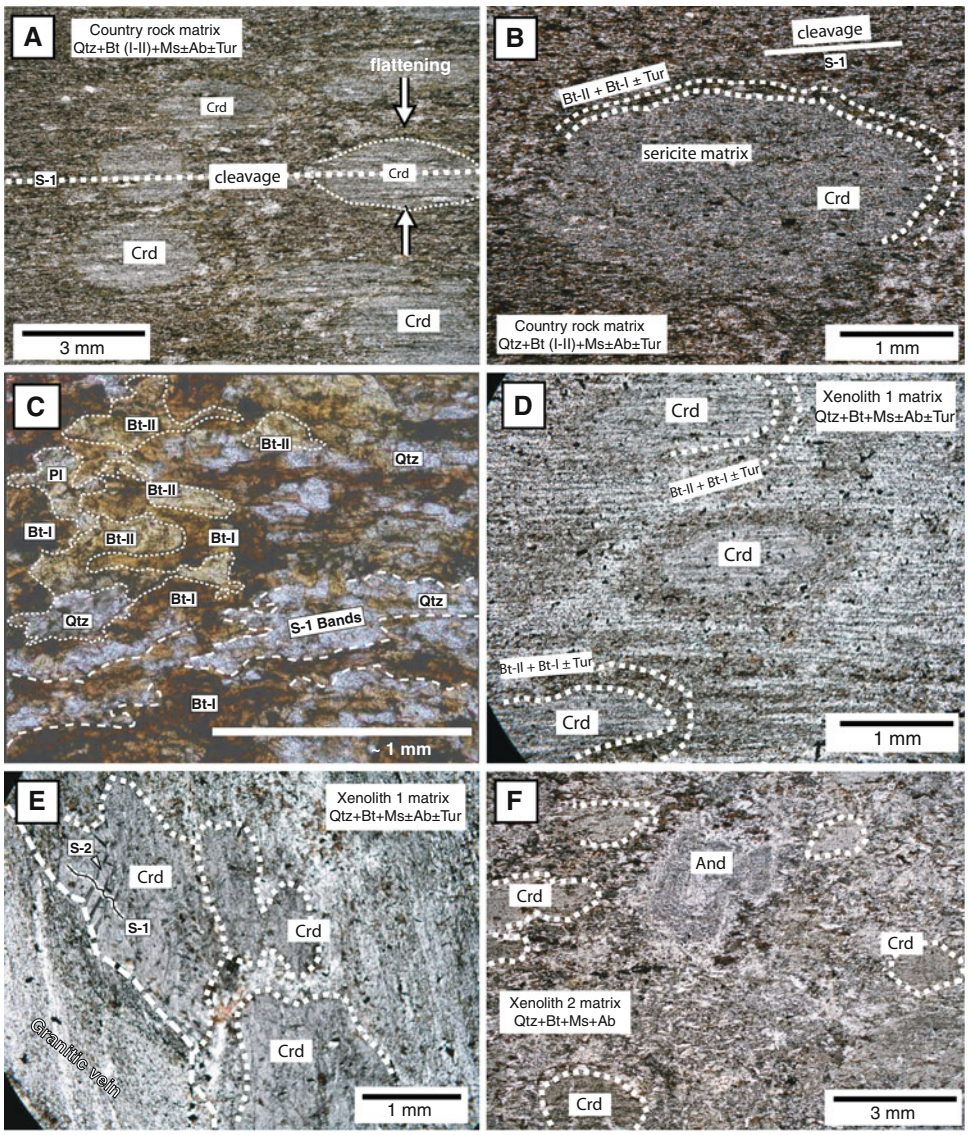

Fig. 4 Transmitted optical microscope photographs of the main metamorphic associations: **a**, **b** and **c** show the texture and mineralogy of the northern country rock schists, characterized by the porphyroblastic growth of cordierite. The matrix is formed by Qtz + Bt (I-II) + Ms ± Tur ± Ab (± Kfs). Two types of biotite (Bt-I and Bt-II) can be identified in the matrix (**c**) and around some Crd coronas. **d** and **e** show Crd-bearing xenoliths with mineralogy very similar to the country rock schists. Corona structures around cordierite are evident in photograph **d**. Photograph **f** shows the metamorphic paragenesis of the xenoliths formed by And + Crd in a matrix of Qtz + Bt + Ms ± Ab (±Kfs)

occurrences can be grouped into: (1) forming bands together with type-I biotites, (2) Bt-II (+ Bt-I ± Tur) at cordierite coronas and replacing cordierite and (3) Bt-II ± Tur in fractures. In most of these occurrences, type-II biotite appears to be in close relationship to type-I. Type-II biotite increases in modal abundance toward the granite contact (Fig. 3b). Beds of Tur + Bt-II-bearing hornfelses have been observed at some locations of the South contact aureole very close to the granite contact (González Menéndez 1998). Part of the Bt-II ± Tur occurrence could be probably related to hydrothermal/magmatic Boron-fluid injections from the granite magma. These B-rich fluids could be responsible for some of the different stages of Bt-II ± Tur growth and the development in the aureole schists. Cordierite associations with Bt-II ± Tur could be in part explained by reactions involving Bt-I + Crd + Boron-rich fluid/melt as described by Wolf and London (1997). Evolved granite and leucogranite magmas, such as the ones in the Nisa-Alburquerque batholith, have low contents in Fe and Mg and could not retain all the B in tourmaline. Therefore, these magmas might have lost a large content of magmatic B to the wall rocks during the final stages of solidification (Morgan and London 1987; Morgan and London 1989; London et al. 1996).

Petrography and mineral assemblages in the xenoliths

Within the granite, the schist xenoliths found show two different types of metamorphic assemblages: type (1) Qtz + Ab + Bt (Bt-II ≥ Bt-I) + Ms + Crd ± Tur schists with equal metamorphic assemblages as the country rock schists (Fig. 4d–e); these xenoliths are the most abundant, being frequently located close to the external contacts of the batholith, especially along the northern contact; they have a wide range of sizes, from diameters less than 1 to 20–30 m (Fig. 2, San Vicente Transect); type (2)

And + Crd schists with the mineral assemblage Qtz + Bt + Ms ± Ab/Kfs + And + pseudomorphs of altered cordierite (Fig. 4f); this type is much less abundant, being usually smaller than type 1 xenoliths (size between 0.5 and 5 m); it appears to be randomly distributed throughout the batholith. Figure 4f shows a xenolith with a metamorphic mineral assemblage of Crd + And. Its matrix mineralogy is composed of Qtz + Bt + Ms + Ab (± Chl in late veins), thus being similar to the rock matrix of the aureole schists, though lacking Bt-II + Tur and depicting a more leucocratic appearance due to the lower modal proportions of biotite crystals (Fig. 4a + b vs f). In this xenolith, cordierite porphyroblasts have rounded shapes, and andalusite crystals are equidimensional. Compared to the aureole schists, this fact could indicate an absence of flattening deformation coeval to this metamorphic assemblage. Cordierite porphyroblasts in Fig. 4f do not show Bt-II + Tur coronas; moreover, andalusite crystals show a well-zoned structure developed over homogeneous nuclei. The absence of tourmaline compared to in situ and other country rock xenoliths could indicate either that the magmatic fluids did not interact with the xenolith or, more probably, that the magmatic fluids entering the xenolith aided through thermal shock fragmentation (Glazner and Bartley 2006) were not B-rich. In summary, we have established a general metamorphic distinction consisting in: (1) Crd-zone assemblages found in the whole aureole and most of the schist xenoliths, and (2) And ± Crd-zone assemblages recognized in a few of the xenolith schists.

Mineral and bulk rock geochemistry

The mineral chemistry is focussed on biotite and cordierite, because in the studied transects they have various textures and mineral chemistries. In general terms, the studied biotites have low Ti contents, higher in type-II and in biotites from the Crd-xenoliths (most of which are also type-II). Biotite values of (Ca + Na + K) are also low, the lowest values belonging to type-I biotites from the country rocks which are, most of them, chloritized. All the biotites have high Al^{6} contents, higher in the type-I from the country rocks, followed by the type-II from the country rocks and by the biotites from the Crd-xenoliths with the lowest contents. All biotite X_{Mg} values are moderate to high (0.39–0.51) (Table 1). Biotites from the Crd-xenoliths are closer to the eastonite–phlogopite/annite end-members compared with those from the country rocks (types I and II), which are in between the phlogopite/annite end-member and muscovite.

Cordierites were analyzed only in the Crd-xenoliths (Table 2) because those from the country rock aureole were mostly replaced by secondary minerals (mainly sericite). The studied cordierites have high X_{Mg} values (0.57–0.59). These X_{Mg} values together with the low Mn contents are typical of metamorphic cordierites (Deer et al. 1997; Erdmann et al. 2004). Channel cations (Ca + Na + K) show very high values (0.13–0.20) causing these Crd to be classified as magmatic cordierites in the Pereira and Bea (1994) diagram.

Plagioclase-feldspars are classified as albites and oligoclases ($Ab_{88–93}$ $Or_{0–0.5}$ $An_{6–14}$). The K-feldspars observed are close to the Or compositional pole ($Ab_{7–12}$ $Or_{88–92}$ An_{0}). Both feldspars have moderate P_2O_5 contents (0.13–0.4 wt%). Tourmalines are classified as intermediate in composition between schorl and dravite and similar to tourmaline from metapelites and metapsammites with a moderate content in Al (Table 3). Accessory phases are Ilm, Hem, Ap, Zrn, Mnz, Xe and sulfides + arsenius.

Temperature estimations were done with the Ti-in-Bt thermometer and the Na-in-Crd thermometer. The application of Ti-in-Bt thermometer (Henry et al. 2005) helped us to distinguish both types of biotites previously described (Fig. 5). The biotites of type-I are thought to be of low temperature (200–360°C) while biotites of type-II are of higher temperature (400–550°C). The Na-in-Crd thermometer: T (±30°C) = [−2744.8 * X_{Na} + 897.4] with X_{Na} = cations per formula unit (Mirwald 1986, Kalt et al. 1998, Dahlquist et al. 2005) has been applied to fresh cordierites from the xenolith (Table 2). Maximum values reached 526–529°C due to the high Na contents present (Table 2). The samples with the highest Na contents (0.15–0.19 c.p.f.u.) were avoided because its projection would be

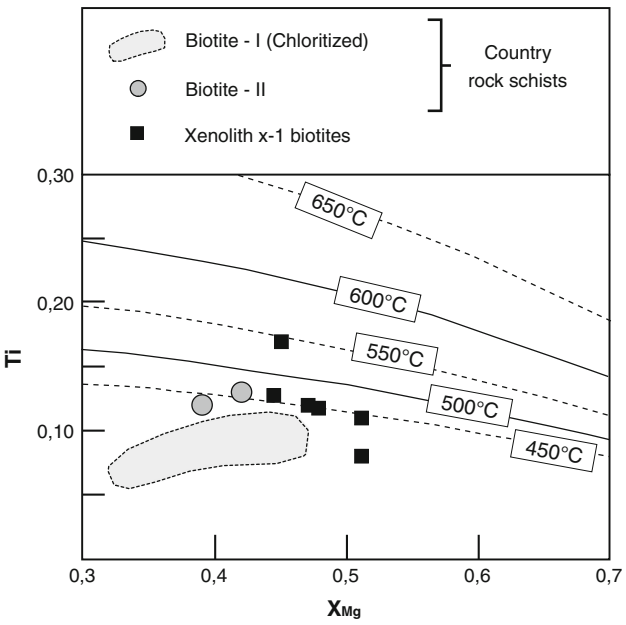

Fig. 5 Mineral chemistry of the country rocks and xenoliths from the Nisa-Alburquerque batholith. Projection of the biotite data on the Ti versus X_{Mg} (Mg/(Mg + Fe)) diagram with the temperature isotherms (°C) from Henry et al. (2005)

far from the experimental conditions from which the thermometer was obtained. Both temperature data from biotites of type-II and from cordierites are in close agreement indicating maximum T of ~550°C. Metamorphic conditions reached in the Variscan regional prograde event were of low grade in the study zone (200–400°C). The thermal input associated with the granite intrusion has been estimated by other studies in 500°C in the country rocks and a minimum of 650°C in the granitic melt. These values are close to the estimated temperatures from the biotites (type-II) and cordierite crystals, and this would relate the development of these minerals (Crd + Bt-II) to the contact metamorphic event. The biotites from the schist xenoliths (Fig. 5) show a widespread from low temperature values, similar to type-I biotites, to higher temperature values similar to type-II biotites. The fact that the xenolith records equivalent temperatures as the country rocks suggests that the incorporation of the xenolith into the granitic magma took place at the very last stages of magmatic cooling and solidification.

Bulk-rock geochemistry of the aureole country rocks shows pelitic/greywacke compositions with variable SiO_2 contents (51–73 wt%) and Al_2O_3 (10–27 wt%). Xenoliths have somewhat higher contents in Al_2O_3, Fe_2O_3 and K_2O compared to the country rocks (Table 4). Acknowledging these differences in bulk rock composition among samples, nevertheless, all of them show very similar immobile element ratios (TiO_2/Al_2O_3 ~ 0.050), suggesting that both country rocks and xenoliths share a similar source rock (Young and Nesbitt 1998) and thus could be grouped into the same formation (the Schist–Greywacke Complex). The projection of the samples in the AFM diagram (Fig. 6) allows us to classify them as high Al pelites with moderate to low Mg contents. We have also projected the average composition of the Schist–Greywacke Complex from López-Munguira et al. (1990), for comparison with our data set. Sample X-2 (Crd + And xenolith) has a higher Al content (27.5 wt%) and lower X_{Mg} values (0.18) compared to the rest of the samples (Crd- xenoliths and Crd-country rocks), and thus, its composition in terms of AFM data is somewhat different. Therefore, we cannot exclude that these differences in bulk rock composition could have been relevant to explain the differences in metamorphic mineral assemblages (Crd + And in type-2 xenoliths vs Crd-bearing country rock schists and type 1-xenoliths).

Thickness and metamorphic grade variation along the contact aureole

There are no changes in the metamorphic assemblage of the country rocks along the northern contact of the batholith. Cordierite is the only contact metamorphic mineral observed. The zone with a slightly higher abundance of

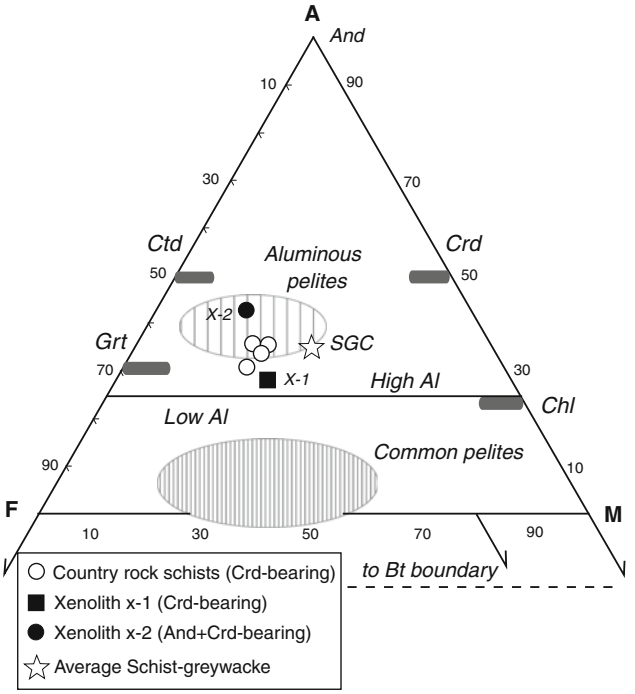

Fig. 6 AFM relationships and plot of the study samples. *Star symbol* represents the average Schist–Greywacke Complex from López-Munguira et al. (1990). The mineral and pelite compositional fields are according to Pattison (2001)

cordierite porphyroblasts occurs in the transect 3 (Valencia de Alcántara) and is located in the middle—eastern part of the batholith (Fig. 2). This fact could reflect a slightly higher metamorphic grade (schist bulk composition is similar to the other transects studied) though the lack of the assemblage Crd + Kfs, or Crd + And, indicates that this possible T increase, if any, must have been very small. Higher-grade (either pressure and/or temperature) assemblages, such as And- or And ± Crd, have been only observed in some xenoliths hosted and surrounded by the granite (González Menéndez 1998).

Regarding outcrop widths of the contact aureole, significant changes are observed along the studied transects. The greatest aureole widths are 1.6–2.6 km in the central and eastern sectors of the batholith. In the central-western sections, the contact aureole varies from 800 m to 1.2 km. The maximum width observed corresponds to the central-eastern sector in transect 3 (Valencia de Alcántara), in which a, hypothetical, slightly higher metamorphic grade was also inferred due to the higher modal proportion of cordierite porphyroblasts.

Zircon saturation temperatures

Regarding magma temperatures, we have obtained zircon saturation temperatures from bulk-rock geochemical data of the coarse-grained granite (González Menéndez 1998,

González Menéndez and Azor 2003). These temperatures were calculated using the equation:

$\ln D^{Zr,\ zircon/melt} = [-3.8 - [0.85(M-1)]] + 12.900/T$, rearranged to yield the temperatures: $T_{Zr} = 12.900/[2.95 + 0.85\ M + \ln(496.000/Zr_{melt})]$; where $M = [(Na + K + 2Ca)/(Al*Si)]$ (Watson and Harrison 1983; Miller et al. 2003). We have generated a simple-isoline contoured map with the zircon saturation temperature values (Fig. 7). These temperatures (~650–750°C) can be considered to be a minimum estimate of magma temperatures at the time of intrusion (Table 5). According to these temperatures, the granites studied would be included in the group of "inheritance-rich, cold granites" of Miller et al. (2003). The highest temperature values are found in easternmost and westernmost domains, while the lowest values are found in the central sectors of the batholith. Some data from the westernmost domains suggest high temperatures (~750°C), but this data set consists only of two samples located close to the southern contact of the batholith. Therefore, this estimation cannot be used to infer high magma temperatures along the northern contact. In conclusion, along the northern contact of the batholith, the magma temperatures at the time of the intrusion/emplacement probably remained between 700 and 750°C. This constant T range probably explains the lack of significant metamorphic grade variations in the country rocks. We have compared graphically the gravimetric data of Azor et al. (2000) with the Zr temperature distribution (Figs. 7a, b). From this comparison, one can observe that the maximum inferred magma temperatures from the eastern domain of the batholith are fairly coincident with a gravity minimum indicative of a significant batholitic root. This correspondence corroborates our basic assumption that higher magma temperatures should be located close to main feeder zones in batholiths and plutons.

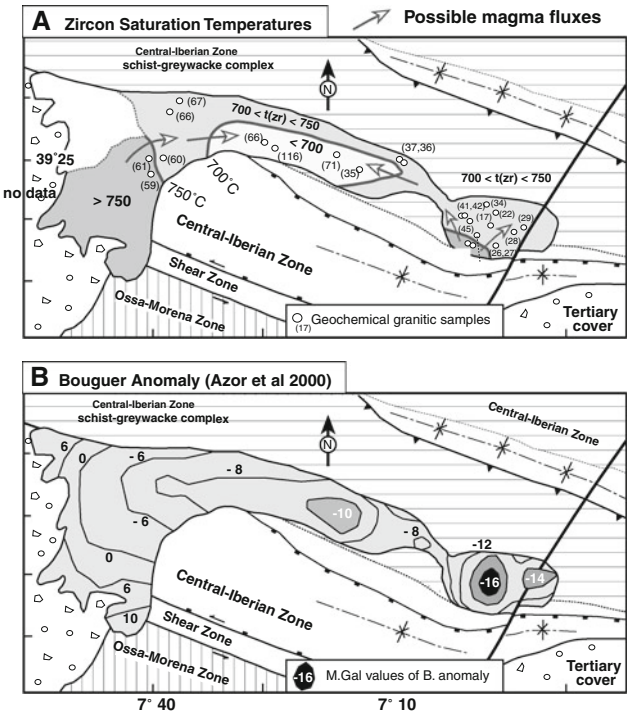

Fig. 7 **a** Geologic scheme and isoline contour map of Zircon Saturation Temperatures obtained from the analytical data (Table 5) of the Nisa-Alburquerque granite (full analytical data set in González Menéndez 1998, 2002 and Ramírez and Menéndez 1999). Most of the magma temperature variations occurred along the southern contact while the temperatures of the northern contact remained nearly constant. **b** Bouguer gravity anomaly map in MGal based on Azor et al. (2000). Lowest values, indicative of a deeper batholith root are located at the eastern zones, where confident maximum T°C (Zr) values are found

Discussion

Differences in metamorphic grade: country rocks versus xenoliths

The differences observed in the metamorphic facies between the country rocks plus most of the xenoliths (Crd-bearing) and the few schist xenoliths with And + Crd might be related to differences in composition, pressure and/or temperature conditions. Compositional differences in the whole-rock Mg/Fe ratio could be important among some of the samples studied. Crd + And xenoliths (X-2 sample) have slightly lower contents in X_{Mg} compared to the Crd-xenoliths (X-1 sample) and country rocks (Table 5). Al contents are also higher in Crd + And xenoliths compared to the rest of the studied rocks. Interestingly, the country rock schists have developed the same metamorphic assemblage (Crd zone) all along the northern batholith contact and their Mg/(Mg + Fe) ratios are similar. Schist xenoliths with the same assemblages (Crd-zone) are thought to be derived from these same country rocks. Despite the above-mentioned compositional differences, Crd + And xenoliths could also have been captured from a formation similar to the northern country rocks (i.e. the Schist–Greywacke Complex) given the similar values of TiO_2/Al_2O_3 ratio in all samples. In summary, xenoliths with the distinctive assemblage And + Crd may be best explained by their slightly lower X_{Mg} bulk rock values that could have promoted the development of And + Crd, instead of Crd-only, through a reaction such as Ms + Chl + Qtz → Crd + And + Bt + H_2O (Pattison and Vogl 2005). Other possibilities could be: (1) development of And + Crd xenoliths from a similar lithology as the northern country rocks, but trapped at slightly higher P conditions (~0.5–1 kbar higher) and brought up by the magma during its ascent; (2) generation of And + Crd xenoliths from a similar lithology as the country rocks, stopped by the granite during its emplacement and heated at

isobaric conditions. In this latter case, the differences in the metamorphic assemblage among xenoliths (Crd vs And + Crd) could be due to the time spent by the xenoliths within the granitic magma and/or to the different sinking depth (deeper xenoliths → higher time spent within the magma → higher heat input → higher T record). These different possibilities are depicted in Fig. 8, which is a schematic P–T diagram of mineral assemblage stabilities in the KFMASH system (after Pattison and Vogl 2005). Comparison of the mineral assemblage studied (Crd-zone) with the mineral stability fields in Fig. 8 suggests that pressure conditions in our case study should have been ≤3 kbar. Previous pressure estimations (González Menéndez and Azor 2003) based on granite Qtz-Ab-Or data plus the coexistence of And + Ms (magmatic) + Tur within the granite, also indicate that the range of pressures for granite emplacement could have been ~2–3 kbar.

Emplacement and structure of the batholith

The maximum widths of the contact aureole correspond to the central-eastern sectors of the batholith, being roughly coincident with the highest magma temperatures. These sectors could represent channels or roots where the main magma flux from lower crustal levels occurred. According to the gravimetric data, the main batholitic root would be located in the eastern sectors, in agreement with metamorphic aureole data and estimated magma temperatures (Zone I of Fig. 9). The central-eastern domain studied in transect 3 (Valencia de Alcántara and Zone II in Fig. 9) records the widest aureole and the highest modal (%) cordierite porphyroblast development, but magma temperatures registered are not very high and gravity data

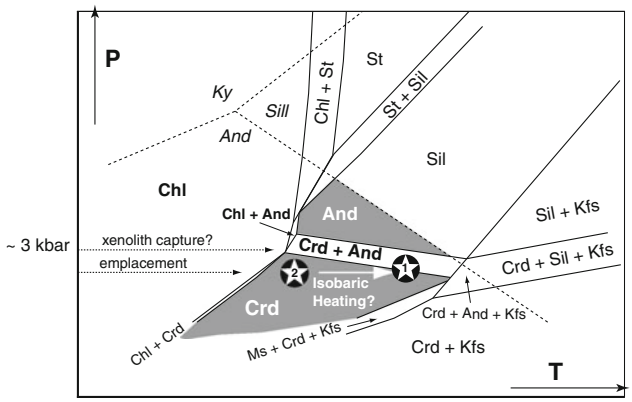

Fig. 8 Schematic P–T representation of mineral assemblage stability fields in the KFMASH system, from Pattison and Vogl (2005). *Star symbols* represent: (*1*) the possible higher pressure stage of xenolith captured by the ascending granite, and (*2*) the final level of emplacement that could have been about 2.5 kbar. An isobaric heating trend linking Crd-country rock schists (+ Crd-xenoliths) and And ± Crd xenoliths could also be possible (*white arrow*)

discard significant roots here. This discrepancy may be explained by the presence of quartz dikes, late fractures and granitic veins in the country rocks at distances of 1.4–2.2 km from the granite contact. This fact suggests that local tectonics could have favored heat transfer from the magma into the country rocks via fractures and injected granitic fluids. Another possible explanation for this discrepancy is to consider this part of the batholith as a zone of significant magma accumulation. This hypothesis is favored by the presence of two granitic facies in the central sector: central granite A and coarse-grained granite, the first one intruding the second one. Furthermore, there is some field evidence indicating an additional later pulse of coarse-grained granite intruded into the central granite A (González Menéndez 1998, 2002; González Menéndez and Azor 2006). Therefore, this sector could have suffered a protracted history of magma accumulation, which, in turn, would have provoked slow magma cooling.

The westernmost sectors of the batholith (Zone III in Fig. 9) show the thinnest aureole widths. Western magma temperatures are as high as in the easternmost sectors, though, as previously discussed, these temperatures are based on only two data. Thus, the temperature of the magmas at the westernmost domains of the northern contact aureole are not well constrained. The gravimetric data indicate that this sector constitutes a relatively thin granite layer, thus precluding important magma accumulation to have occurred here. Therefore, a thin contact aureole agrees well with gravimetric data. No magma conduits have been detected by gravimetry, but magma intrusions necessarily took place in order to explain the presence of the late central granite B and the central granite A, both intruding into the coarse-grained granite. The conduits for ascent were probably narrow enough for being undetectable by gravimetric surveys (Vigneresse 1990). Therefore, we envisage in the western sector of the Nisa-Alburquerque batholith a scenario of small magma volumes represented by a thin layer of the coarse-grained granite heated with small intrusions of central granite B (granodiorites–tonalites). These mafic compositions would represent higher temperature melts injected in the magma mush of the coarse-grained granite and possibly rising its temperature in some specific locations where these intrusions took place (Solá 2007). This might help to explain the recorded T(Zrn) ≈ 750°C obtained at some places of these western domains.

Conclusions

The studied contact metamorphic aureole shows significant differences in thickness along the northern contact of the batholith, which can be correlated with different magma

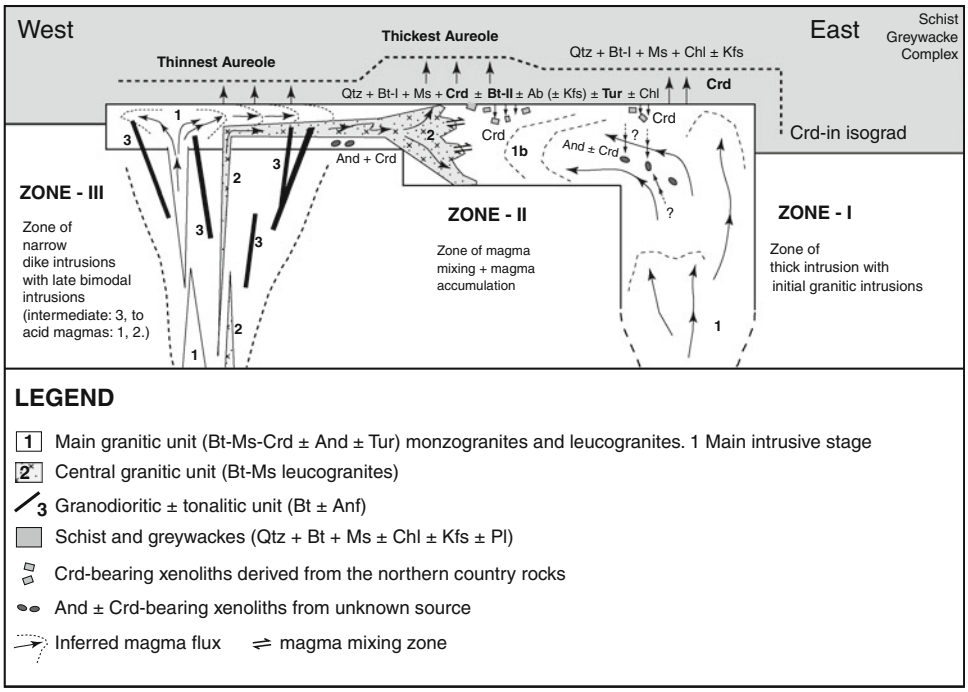

Fig. 9 Schematic model showing possible zones of intrusion and magma flow, based on petrological–geochemical–gravimetric data plus data from the contact aureole and xenoliths. The batholith is divided into three different zones, which correspond to different processes and internal structure. From East to West: *Zone I* corresponds to the root of the main intrusion, leading to the development of a thick contact aureole; *Zone II* is a zone with magma accumulation and development of the widest contact aureole; *Zone III* is interpreted as a thinner magma chamber feeded by dykes, where a narrow contact aureole was developed

chamber architecture and magmatic processes. Metamorphic grade reached in the country rocks defines a Crd-zone with maximum temperatures of ~550°C (Bt and Crd thermometers). Granitic magma in contact with the country rocks was initially at 700–750°C (probably closer to the lower value) and pressures between 2 and 3 kbar.

The emplacement mode outlined in this work for the Nisa-Alburquerque batholith (Fig. 9) is based on three mutually independent sources of data: contact aureole data, petrology-geochemistry of the granitic rocks and gravimetric data. We propose the existence of a main feeding root located at the eastern sectors of the batholith (Zone I). This eastern feeder helps to explain the higher magmatic temperatures recorded here and the wider contact aureole development. In the westernmost sectors (Zone III), magma volume would be lower, giving way to a relatively thin granite sheet. Nevertheless, intrusions injected through narrow conduits would have taken place in these western sectors (secondary feeders), generating mainly the central granite B and the central granite A and keeping local high magma temperatures. This fact can explain the somewhat narrower contact aureole in the western sector, but maintaining the same metamorphic grade as in the central-eastern sectors. Finally, the central domain of the batholith (Zone II) seems to be a zone where the evolved magma fluxes from the east and from the west encountered and interacted, making cooling of granite magma slower than in other parts of the batholith (González Menéndez and Azor 2006). This would help to explain the greater thickness of the metamorphic contact aureole developed, without a significant change in the metamorphic grade.

Schists xenoliths trapped within the granite show two different metamorphic assemblages: (1) Crd-bearing schists, located close to the northern granite contact, having the same metamorphic grade as the country rocks and probably trapped from these same country rocks at the present emplacement level; (2) a small group of And + Crd-bearing schists, which are smaller and much less abundant. Given the differences in bulk rock composition between And + Crd xenoliths, Crd-bearing xenoliths and country rocks, the development of the And + Crd metamorphic assemblage could be due to the slightly lower X_{Mg} values of these xenoliths. Other less probable possibilities could be xenolith entrapment at the emplacement level followed by isobaric heating or xenolith capture at slightly higher pressure conditions ($\approx$ 0.5–1 kbar higher than the final emplacement level).

Acknowledgments We thank Jose María Toyos and Augusto Rodríguez García for discussions and text corrections on a preliminary manuscript. We appreciate and thank the critical and constructive reviews made by Dr. Bernardo Cesare and Dr. Javier Escuder-Viruete that led to a significant improvement of this paper. We also thank Dr. Wolf-Christian Dullo and Dr. Ingo Braun for the editorial handling of the manuscript. This research has been financed by the Spanish Ministry of Science and Innovation through grants CGL2007-63101/BTE and TOPO-IBERIA CONSOLIDER-INGENIO 2010 CSD2006-00041.

References

Aranguren A, Larrea FJ, Carracedo M, Cuevas J, Tubía JM (1997) The Los Pedroches batholith (Southern Spain): poliphase interplay between shear zones in transtension and setting of

granites. In: Bouchez JL, Hutton DHW, Stephens WE (eds) Granite: from segregation of melt to emplacement fabrics. Kluwer Academic Publishers, Dordrech, pp 215–229

Aranguren A, Cuevas J, Tubia JM, Roman-Berdiel T, Casas-Sainz A, Casas-Ponsati A (2003) Granite laccolith emplacement in the Iberian arc: AMS and gravity study of the La Tojiza pluton (NW Spain). J Geol Soc London 160:435–445

Arenas R, Farias P, Gallastegui G, Gil Ibarguchi JI, Gonzalez Lodeiro F, Klein E, Marquínez J, Martín Parra LM, Martínez Catalán JR, Ortega E, Pablo Macía JG, Peinado M, Rodríguez-Fernández LR (1988) Características geológicas y significado de los dominios que componen la Zona de Galicia Tras-os-Montes. II Congreso Geológico de España. Simposios, pp 75–84

Azor A, Menéndez LG, Galindo-Zaldivar J, Galadí-Enriquez E (2000) The structure of the Nisa-Alburquerque batholith (SW Iberian Massif). Variscan-Appalachian dynamics. 15th international conference on basement tectonics. La Coruña, Spain. Abstracts 49–50

Azor A, Expósito I, González Lodeiro F, Simancas JF, Martínez Poyatos D (2004) La Unidad Central o contacto entre las zonas de Ossa-Morena y Centroibérica. Geología de España SGE-IGME, Madrid, pp 128–133

Baxter EF (2003) Natural constraints on metamorphic reaction rates. Geochronology: linking the isotopic record with petrology and textures. Geol Soc Spec Publ 220:183–202

Bea F (2004) La naturaleza del magmatismo de la Zona Centroibérica: consideraciones generales y ensayo de correlación. En Geología de España (JA Vera Ed) SGE-IGME Madrid, pp 186–188

Bea F, Sánchez González de Herreo JG, Serrano Pinto M (1987) Una compilación geoquímica para los granitoides del Macizo Hespérico. En: Geología de los granitoides y rocas asociadas del Macizo Hespérico. Bea F, Carnicero A, Gonzalo JC, López plaza M, Rodríguez Alonso MD, pp 87–193

Gumiel P, Campos R, Monteserín V, Bellido F (2002) Mapa Geológico y de Recursos Minerales del Sector Centro-Occidental de Extremadura (E. 1: 100,000). In: Junta de Extremadura Special Report. IGME-CIEMAT

Bucher K, Frey M (2002) Petrogenesis of metamorphic rocks. Springer, Berlin

Campos R, Plata JL (1991) Gravity Survey. In: Development of new multidisciplinary techniques for mineral exploration in several areas of the western Iberian peninsula. In: Gumiel P, Pacheco A, Campos R (eds). ITGE Special Publication, pp 55–66

Casquet C, Galindo C (2004) Magmatismo varisco y postvarisco en la Zona de Ossa-Morena. En Geología de España. In: Vera JA (ed) SGE-IGME, Madrid, pp 194–198

Castro A, Corretgé LG, De la Rosa JD, Enrique P, Martínez FJ, Pascual E, Lago M, Arranz E, Galé C, Fernández C, Donaire T, López S (2002) Paleozoic magmatism. In: Gibbons W, Moreno T (eds) The Geology of Spain. Geological Society, London, pp 117–153

Dahlquist JA, Rapela CW, Baldo EG (2005) Petrogenesis of cordierite-bearing S-type granitoids in Sierra de Chepes, Famatinian orogen, Argentina. J South Am Earth Sci 20:231–251

Deer WA, Howie RA, Zussman J (1997) Rock-forming minerals. Disilicates and ring silicates, vol 1B, 2nd edn. Geological Society, London, pp 135–232

Erdmann SA, Clarke DB, MacDonald MA (2004) Origin of chemically zoned and unzoned cordierites from the South Mountain and Musquodoboit batholiths. Trans Roy Soc Edinb Earth Sci 95:99–110

Farias P, Gallastegui G, González Lodeiro F, Marquínez J, Martín Parra LM, Martínez Catalán JR, Pablo Macía JG, Rodríguez-Fernández LR (1987) Aportaciones al conocimiento de la litoestratigrafía y estructura de Galicia Central. Mem Museo e Lab Miner Geol, Fac Ciencias, Univ Porto 1:411–431

Galadí-Enríquez E, Galindo-Zaldívar J, Simancas JF, Expósito I (2003) Diapiric emplacement in the upper crust of a granitic body: the La Bazana granite (SW Spain). Tectonophysics 361:83–96

Galindo C, Casquet C (2004) Magmatismo prevarisco de la Zona de Ossa-Morena. Geología de España, SGE-IGME, Madrid, pp 190–194

Glazner AF, Bartley JM (2006) Is stoping a volumetrically significant pluton emplacement process? GSA Bull 118(9/10):1185–1195

González Menéndez L (1998) Petrología y Geoquímica del Batolito de Nisa-Alburquerque. PhD thesis, Universidad de Granada, Spain

González Menéndez L (2002) Petrología del Batolito de Nisa-Alburquerque. Rev Soc Geol España 15(3–4):233–246

González Menéndez L, Azor A (2003) Condiciones PT de emplazamiento del Batolito de Nisa-Alburquerque. Geogaceta 34:103–106

González Menéndez L, Azor A (2006) Estructura interna del Batolito de Nisa-Alburquerque. Geogaceta 40:131–134

González Menéndez L, Bea F (2004) El batolito de Nisa-Alburquerque. Geología de España, SGE-IGME, Madrid, pp 120–122

Henry DR, Guidotti CV, Thompson JA (2005) The Ti-saturation surface for low to medium pressure metapelitic biotites: implications for geothermometry and Ti-substitution mechanism. Am Mineral 90:316–328

Jaeger JC (1968) Cooling and solidification of igneous rocks. In: Hess HH, Poldervaart A (eds) Basalts: the Poldervaart treatise on rocks of basaltic composition, vol 2. Interscience Publishers, Wiley, New York, pp 503– 536

Julivert M, Marcos A, Truyols J (1972) Lévolution paleogeographic du NW de l'Espagne pendant l'Ordovicien-Silurien. Bull Soc Geol Mineral Bretagne 4:1–7

Kalt A, Altherr R, Ludwig T (1998) Contact metamorphism in pelitic rocks on the Island of Kos (Greece, Eastern Aegean Sea): a test for the Na-in-cordierite thermometer. J Petrol 39(4):663–688

Kretz R (1983) Symbols for rock-forming minerals. Am Mineral 68:277–279

London D, Morgan GB IV, Wolf M (1996) Boron in granitic rocks and their contact aureoles. In: Grew ES, Anovitz L (eds) Boron: mineralogy, petrology and geochemistry in the Earth′s crust. Min Soc Am Reviews in Mineralogy 33:719–734

López-Munguira A, Sebastián Pardo E, Nieto García F (1990) Mineralogía y Geoquímica del límite entre las zonas de Ossa-Morena y Centroibérica en el area extremeña del Macizo Hespérico. Rev Soc Geol España 3(1–2):43–51

López-Munguira A, Nieto García F, Sebastián Pardo E, Velilla N (1991) The composition of phyllosilicates in Precambrian, low-grade-metamorphic, clastic rocks from the Southern Hesperian Massif (Spain) used as an indicator to metamorphic conditions. Precambrian Res 53:267–279

Lotze F (1945) Zur Gliederum der Varisziden der Iberischen Meseta. Geotekt Forsch 6:78–92

Mather JD (1970) The biotite isograd and the lower greenschist facies in the Daldarian rocks of Scotland. J Petrol 11:253–275

Miller CF, Meschter McDowell S, Mapes RW (2003) Hot and cold granites? Implications of zircon saturation temperatures and preservation of inheritance. Geology 31(6):529–532

Mirwald PW (1986) Ist cordierit ein geothermometer. Fortschritte der Mineralogie 64(Beiheft 1):119

Morgan GB IV, London D (1987) Alteration of amphibolitic wallrocks around the Tanco rare-element pegmatite, Benic Lake, Manitoba. Am Mineral 72:1097–1121

Morgan GB IV, London D (1989) Experimental reactions of amphibolite with boron-bearing aqueous fluids at 200 Mpa: implications for tourmaline stability and partial melting in mafic rocks. Contrib Mineral Petrol 102:281–297

Pattison DRM (2001) Instability of Al_2SiO_5 "triple-point" assemblages in muscovite + biotite + quartz-bearing metapelites, with implications. Am Mineral 86:1414–1422

Pattison DRM, Harte B (1997) The geology of the Ballachulish igneous complex and aureole. Scotish J Geol 33(1):1–29

Pattison DRM, Vogl JJ (2005) Contrasting sequences of metapelitic mineral-assemblages in the aureole of the tilted Nelson Batholith, British Columbia: implications for the phase equilibria and pressure determination in andalusite-sillimanite settings. Can Mineral 43:51–88

Pattison DRM, Spear FS, Debuhr CL, Cheney JT, Guidotti CV (2002) Thermodynamic modelling of the reaction muscovite + cordierite = Al_2SiO_5 + biotite + Quartz + H_2O: constraints from natural assemblages and implications for the metapelitic petrogenetic grid. J metamorphic Geol 20:99–118

Pereira MD, Bea F (1994) Cordierite producing reactions in the Peña Negra complex, Central Spain, Avila Batholith, Central Spain: the key role of cordierite in low pressure anatexis. Can Mineral 32:763–780

Ramírez JA, Menéndez LG (1999) A geochemical study of two peraluminous granites from south-central Iberia: the Nisa-Alburquerque and Jalama batholiths. Min Mag 63(1):85–104

Ramsay JG (1989) Emplacement kinematics of a granite diapir: the Chindamora batholith, Zimbabwe. J Struct Geol 11:191–209

Rodríguez Alonso MD, Diez Balda MA, Perejón A, Pieren A, Liñan E, López Diaz F, Moreno F, Gámez Vintaned JA, González Lodeiro F, Martínez Poyatos D, Vegas R (2004) Dominio del Complejo Esquisto Grauváquico: Estratigrafía. La secuencia litoestratígráfica del Neoproterozoico—Cámbrico Inferior. In: Vera JA (ed) Geología de España. SGE-IGME, Madrid, pp 78–81

Rodríguez Fernández LR, Bellido F, Díez A, González Clavijo E, Heredia N, López F, Marín C, Martín-Parra LM, Martín-Serrano A, Matas J, Montes M, Nozal F, Quintana L, Roldán F, Rubio F, Salazar A (2004) Mapa Tectónico de España a escala 1: 200.000. In: Vera JA (ed) Geología de España. SGE-IGME, Madrid

Rodríguez Suárez JI (1985) Petrografía, Blástesis, y Deformación en la Aureola de Contacto del plutón de Nisa-Alburquerque. M.SC thesis. Universidad de Oviedo, Spain

Romeo I, Capote R, Tejero R, Lunar R, Quesada C (2006) Magma emplacement in transpression: the Santa Olalla Igneous Complex (Ossa-Morena Zone, SW Iberia). J Struct Geol 28:1821–1834

Simancas JF, Galindo-Zaldívar J, Azor A (2000) Three-dimensional shape and emplacement of La Cardenchosa deformed pluton (Variscan Orogen, southwestern Iberian Massif). J Struct Geol 22:489–503

Simancas JF, Martínez Poyatos D, Expósito I, Azor A, González Lodeiro F (2001) The structure of a major suture zone in the SW Iberian Massif: the Ossa-Morena/Central Iberian contact. Tectonophysics 332:295–308

Solá RA (2007) Relaçoes Petrogeoquímicas Dos Maciços Graníticos do NE Alentejano. PhD thesis. University of Coimbra, Portugal

Solá RA, Williams IS, Neiva AMR, Ribeiro ML (2009) U-Th-Pb SHRIMP ages and oxygen isotope composition of zircon from two contrasting late variscan granitoids, Nisa-Albuquerque batholith, SW Iberian Massif: petrologic and regional implications. Lithos 111:156–167

Vigneresse JL (1990) Use and misuse of geophysical data to determine the shape at depth of granitic intrusions. Geol J 25:249–260

Vigneresse JL, Bouchez JL (1997) Successive granitic magma batches during pluton emplacement: the case of Cabeza de Araya (Spain). J Petrol 38(12):1767–1776

Watson EB, Harrison TM (1983) Zircon saturation revisited: temperature and composition effects in a variety of crustal magma types. Earth Planet Sci Lett 64:295–304

Wolf BM, London D (1997) Boron in granitic magmas: stability of tourmaline in equilibrium with biotite and cordierite. Contrib Mineral Petrol 130:12–30

Yardley BWD (1989) Metamorphic petrology. Longman Earth Sciences Series, England

Yenes M, Álvarez F, Gutierrez-Alonso G (1999) Granite emplacement in orogenic compressional conditions: the La Alberca-Bejar granitic area (Spanish Central System, Variscan Iberian Belt). J Struct Geol 21:1419–1440

Young GM, Nesbitt HW (1998) Processes controlling the distribution of Ti and Al in weathering profiles, siliciclastic sediments and sedimentary rocks. J Sediment Res 68(3):448–455